

Anticancer Effect and Safety Profile of a 4-Pyridyl Linked Triazolotriazine Derivative against Colorectal Tumor

R. Monfared¹, S. Farzipour^{2,3}, S. Dadashpour¹, Z. Zakeri Khatir¹, S. J. Hosseinimehr^{3*}, F. Talebpour Amiri⁴, H. Irannejad^{1†}

¹ Department of Medicinal Chemistry, Faculty of Pharmacy, Mazandaran University of Medical Sciences, Sari, Islamic Republic of Iran

² Cardiovascular Diseases Research Center, Department of Cardiology, Heshmat Hospital, School of Medicine, Guilan University of Medical Sciences, Rasht, Islamic Republic of Iran

³ Department of Radiopharmacy, Faculty of Pharmacy, Mazandaran University of Medical Sciences, Sari, Islamic Republic of Iran

⁴ Department of Anatomy, Faculty of Medicine, Molecular and Cell Biology Research

Received: 2 October 2023 / Revised: 5 November 2023 / Accepted: 28 November 2023

Abstract

Cancer is the second leading cause of global death, and colorectal cancer is the fourth most common cancer worldwide. In this study, the anticancer effect and safety profile of a 3-(pyridyl-4-l-methylthio) triazolotriazine derivative (**10b**) was investigated. The anti-tumor activity of **10b** was evaluated on HT-29 human colon cancer cell. To confirm the *in vivo* anti-cancer effect of **10b**, human colon tumor xenograft mice was used. Tumor bearing mice were treated with **10b** and paclitaxel for 10 days, then were sacrificed and their heart, liver and tumor tissues were isolated for pathological evaluation. Mice weight and tumor size were measured daily, and mortality was recorded. The results of cellular experiments showed that IC₅₀ of paclitaxel and **10b** was 0.34 and 8.92 μM after 72 hours, respectively. The results of measuring the weight of mice and tumor size didn't show any significant changes in the **10b** treated groups. Pathological examinations indicated that the extent of hepatotoxicity and cardiac toxicity in mice receiving **10b** was lower than that of the paclitaxel group. Interestingly and hopefully, all mice treated with **10b** remained alive during the experiment but 50% of mice treated with paclitaxel and also 50% of mice in the control group were died. Totally, **10b** showed acceptable *in vitro* anti-tumor activity on HT-29 colorectal cells and no mortality in this group confirms the safety profile of **10b**.

Keywords: Colorectal cancer; Triazolotriazine; Tumor; HT-29; Xenograft.

Introduction

Cancer is the second leading cause of death in the world (1). In 2020, almost 19.3 million new cancer cases and almost 10.0 million cancer deaths occurred Worldwide (2). Cancer is a general term used for a range of dangerous diseases; which may affect different parts of the body. The disease is characterized by a

rapid and uncontrolled formation of abnormal cells. The abnormal cells may cause a tumor or gland to form an abnormal mass in other parts of the body. If this process is not stopped, the complication may progress to the point where it causes the death of an organ (3).

The main treatments for cancer are often surgery, radiotherapy and chemotherapy. Pharmacological agents often provide temporary relief from symptoms,

* Corresponding author: Tel: 09113210663; Email: sjhosseinim@yahoo.com, sjhosseinim@mazums.ac.ir

† Corresponding author: Tel: 09124572673; Email: irannejadhamid@gmail.com

longevity, and sometimes complete recovery. In recent years, a large number of anti-cancer drugs have been identified and developed; But they have many side effects. Therefore, it is necessary to try to find anti-cancer agents with better safety profile and reduced toxicity (4).

Colorectal cancer (CRC) is a heterogeneous disorder with disease-related overlapping subgroups, which may be recognized in primary tumors, primary cultures, xenografts, and traditional cell lines. This disease, also known as bowel, colon, or rectal cancer, ranks among the most common solid tumors worldwide. Most colorectal cancers are caused by aging and lifestyle factors, with only a few cases caused by underlying genetic disorders. Cancer-related mortality is strongly influenced by the high potential of metastasis and drug resistance (5, 6).

Studies on the regulation of signal transduction pathways in normal and malignant cells have provided important information on the mechanisms of oncogenesis and tumor progression. Today, more than 75 types of human tyrosine kinase (RTK) receptors are known, and many of them are involved in oncogenesis. Some types of tyrosine kinase receptors are proto-oncogenes that are involved in all main tumor growth and metastasis events, such as changes in reactive oxygen species, activation of downstream signal transduction molecules, cell proliferation, migration, and survival. Tyrosine kinase receptors are key molecular targets for designing anticancer drugs (7–10).

One of the most important types of these receptors is hepatic growth factor receptor (HGFR), also known as receptor tyrosine kinase c-Met which mediates a diverse set of normal physiological process such as morphogenesis, angiogenesis, proliferation, survival and apoptosis. Aberrant or amplification of HGF/c-Met signaling pathway has been associated with metastatic progression, invasion and developing resistance against the conventional therapies. Therefore, inhibition of this target is a promising strategy in a group of anticancer drugs (11).

Recently, in a research on the design and synthesis of specific c-Met kinase inhibitors, we found compounds with the core structure of triazolotriazine, which showed promising in vitro anti-cancer effect on some tumor cell lines and nanomolar IC_{50} values for the inhibition of the c-Met enzyme (12). Of the several dozen compounds studied, compound 10b was more effective than its congeners with IC_{50} values of 0.74 and 1.14 μ M on HepG2 and A-549 cell lines respectively and an IC_{50} of 4.6 nM towards the inhibition of the c-Met enzyme (Figure 1).

Considering the remarkable suppressive effects of

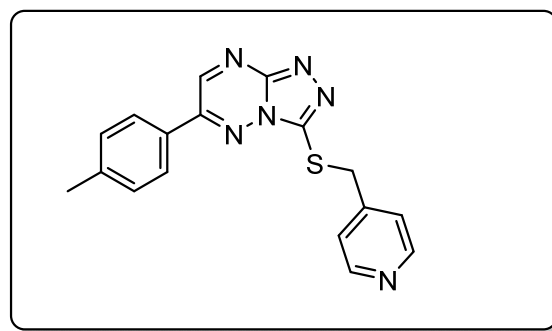


Figure 1. The structure of 3-((Pyridin-4-ylmethyl)thio)-6-(p-tolyl)-[1,2,4] triazolo[4,3-b] [1,2,4] triazine (10b) as a potent c-Met kinase inhibitor.

10b on the tumor cells previously reported; in the current study, we aimed at evaluating the in vitro and in vivo potential of 10b on the HT-29 tumor cells xenografted nude-mice compared to paclitaxel and investigating its organ and tissue toxicity as well as survival and mortality of the mice.

Materials and Methods

In this study, the HT-29 cell line (human colon cancer cells) was purchased from the Pasteur Institute and stored in liquid nitrogen. The cells were cultured in DMEM medium containing 10% fetal bovine serum (FBS), penicillin-streptomycin at 37°C in an atmosphere with 5% CO_2 concentration. Compound 10b was previously synthesized in our lab (12) and paclitaxel was prepared as an injectable liquid at a concentration of 6 mg/ml (Sobhan Pharmaceutical Company, Iran).

In vitro study

MTT assay was performed in order to compare the cytotoxic effect of 10b and paclitaxel on HT-29 colon cancer cells and to determine the IC_{50} values. This test was performed simultaneously on two 96-well plates, whereas 10,000 cells were added to each well in each 96-well plate. The 96-well plates containing the implanted cells were then incubated for 24 hours to allow the cells to reach their logarithmic growth stage. The new culture medium without drugs was added to rows 1 and 7 as control group. In rows 2 to 6, culture medium containing paclitaxel at concentrations of 0.01, 0.05, 0.1, 0.5 and 1 μ M, and in rows 8 to 12, culture medium containing 10b at concentrations of 0.5, 1, 5, 10 and 50 μ M were added. One plate was then incubated for 48 hours and the other plate for 72 hours to allow the cells to be in sufficient contact with the drugs. After incubation, the culture was removed and 20 μ l of MTT solution with fresh culture medium was added to each

well, and 96-well plates were placed in the incubator for 4 hours. After that, 100 μ l of DMSO solution was added to each well (to dissolve insoluble formazan). It was then mixed for 15 minutes to completely dissolve the formazan. The absorbance of each well was read with an ELISA Reader at 570 / 630 nm (Bioteck, USA). Cells without any treatment were used as control for comparison of absorbance and cell viability (13).

$$\% \text{ Viability} = \frac{\text{OD mean (Treated Well)}}{\text{OD mean (Control Well)}} \times 100$$

OD= optical density

Animal study

The experiments were approved by the Ethical Committee of Mazandaran University of Medical Sciences (ID#IR.MAZUMS.REC.1397.4831). In this study, 30 nude mice in the weight range of 18-22 g and in the age range of 6 to 8 weeks were purchased from Pasteur Amol Institute (IRAN). The mice were kept under standard conditions with sterile water and food. HT-29 tumor cells were injected intraperitoneal at a rate of 5×10^6 per mouse. The tumor was allowed to grow for 2 to 3 weeks, and when the tumor size reached 350-450 mm^3 , in vivo testing was started. Tumor size was calculated by the $(\text{length} \times \text{width}^2 \times 0.5)$ formula. All experiments were performed under a laminar hood and in an aseptic environment.

Mice were divided into three groups: control, paclitaxel and 10b (n= 10). The control group received solvent for ten days. The paclitaxel group received paclitaxel with a concentration of 5 mg/kg for five days and after two days of resting, the second injection was performed and continued to the end of the experiment. The 10b group received the synthesized 10b at a dose of 20 mg/kg at similar schedule injection to paclitaxel. Mice mortality, weight, and tumor size were measured daily.

Histopathological examinations

Tumor, heart and liver tissues were fixed in 10% formalin buffer. The fixed tissue was dehydrated in a series of stratified alcohols, clarified in xylene, and molded vertically in paraffin. Sections of 5 μ m-thick were prepared using rotating microtome, and used for histopathological evaluation. Semi-quantitative tissue damage for each slide were considered on a scale of 0 (normal), 1 (mild), 2 (low), 3 (moderate) and 4 (severe) (14).

Statistical analysis

All data were evaluated by Graphpad prism software (USA). All data were expressed as mean \pm standard deviation. $P < 0.05$ was accepted as a statistically

significant change.

Results

MTT assay

The percentage of cell survival against different concentrations of paclitaxel is shown in Figure 2. As illustrated in the Figure 2, the rate of cell mortality increases with higher concentrations of paclitaxel and also after passing 72 h of the drug treatment. The highest toxicity was observed in the group containing paclitaxel at the dose of 1000 nM after 72 hours and the lowest mortality rate belonged to the group receiving 10 nM after 48 hours. After 48 hours, the cytotoxic effect of paclitaxel in HT-29 cells was calculated as an IC_{50} value of $0.86 \pm 0.18 \mu\text{M}$ and after 72 hours it was $0.34 \pm 0.09 \mu\text{M}$.

The percentage of cell survival in different concentrations of 10b is shown in Figure 3. As represented, the cell mortality rate was the highest in the group containing 10b at a dose of 50 μM , and after 72 hours of the drug treatment. Among the groups receiving 10b, the lowest mortality rate belonged to the group receiving 0.5 μM dose after 48 hours. Accordingly, increasing the drug concentration increased the cytotoxicity of 10b. IC_{50} of the cytotoxic effect of 10b in HT-29 tumor cells was calculated and was shown to be $17.50 \pm 5.22 \mu\text{M}$ after 48 hours and $8.92 \pm 2.35 \mu\text{M}$ after 72 hours of the treatment.

Animal experiments

Body weight

The weight of mice in the three groups were recorded daily during the treatment period and the corresponding variation curves are represented in Figure 4. As illustrated, the weight of mice in control and 10b groups was associated with a slight increase until day 3 and after that remained relatively constant. Mice in the paclitaxel group lost weight in the fifth and sixth day of the treatment, although the difference in weight of mice between the three groups was not statistically significant.

Tumor size

According to the represented data in Figure 5, the size of tumors in the control and paclitaxel groups changed similarly during the treatment and totally was associated with a slight increase at the end of the treatment. In the case of 10b, the volume of tumors increased constantly during the study, although the difference in tumor size between the three groups was not statistically significant.

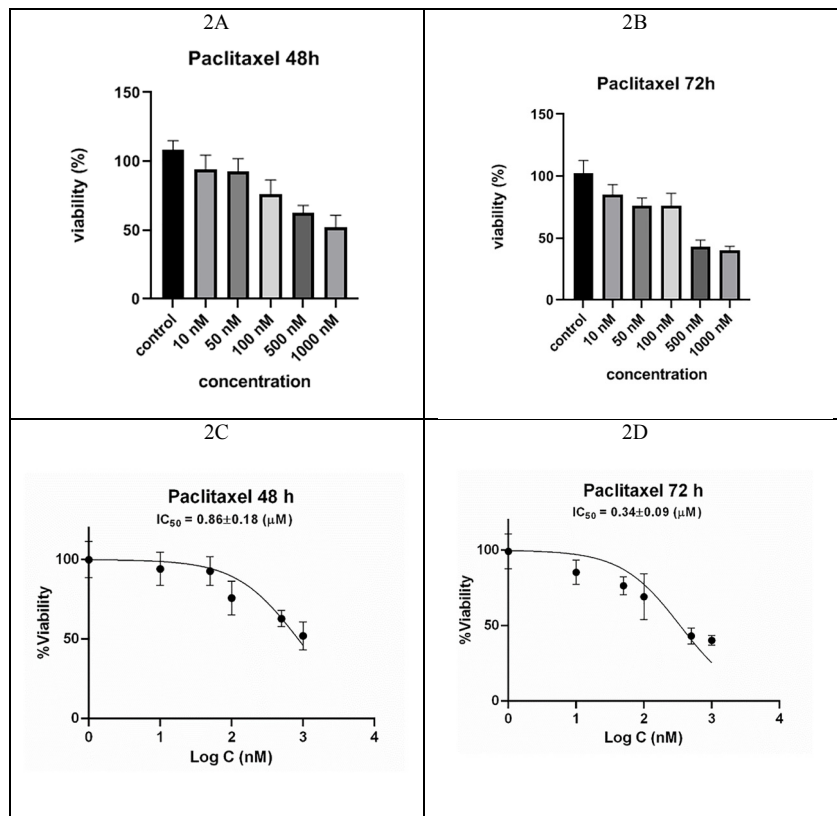


Figure 2. Cell viability percentage exposed to different doses of paclitaxel, A) after 48 and B) after 72 hours and the corresponding IC₅₀ value curves C and D.

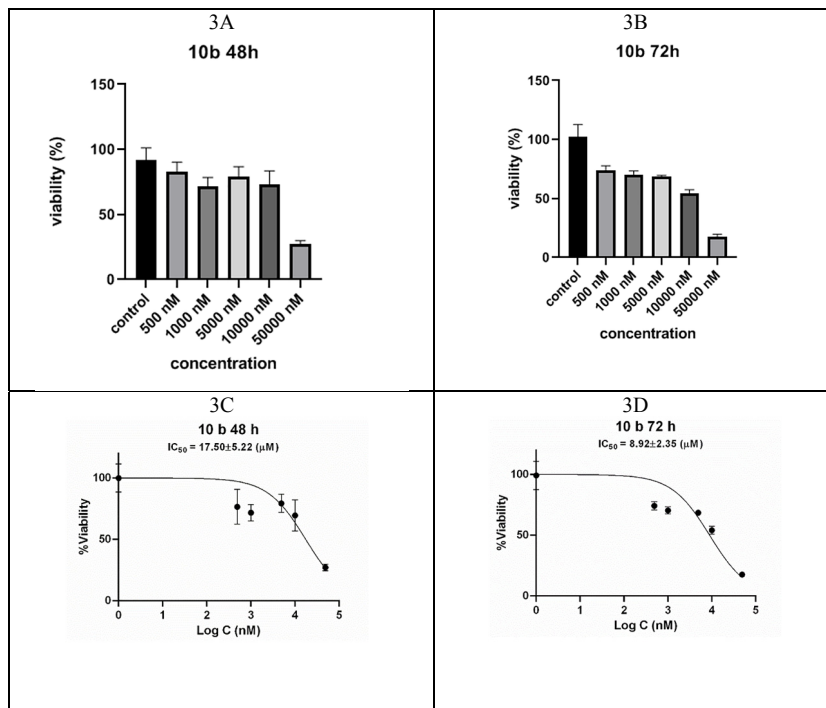


Figure 3. Cell viability percentage exposed to different doses of 10b, A) after 48 and B) after 72 hours. IC₅₀ curves of 10b against HT-29 cell line after 48 (C) and 72 hours (D).

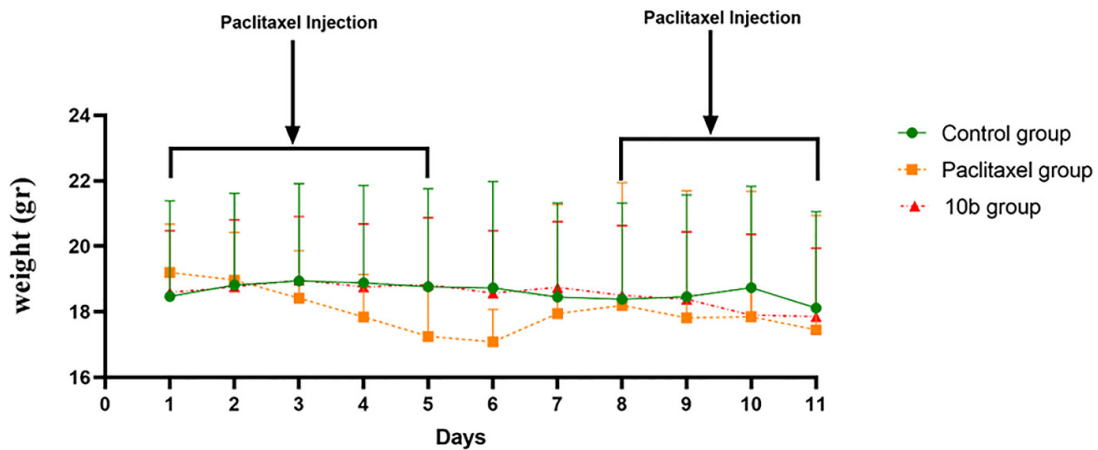


Figure 4. The results of measuring the weight of mice in different groups during the treatment period (Mean \pm SE).

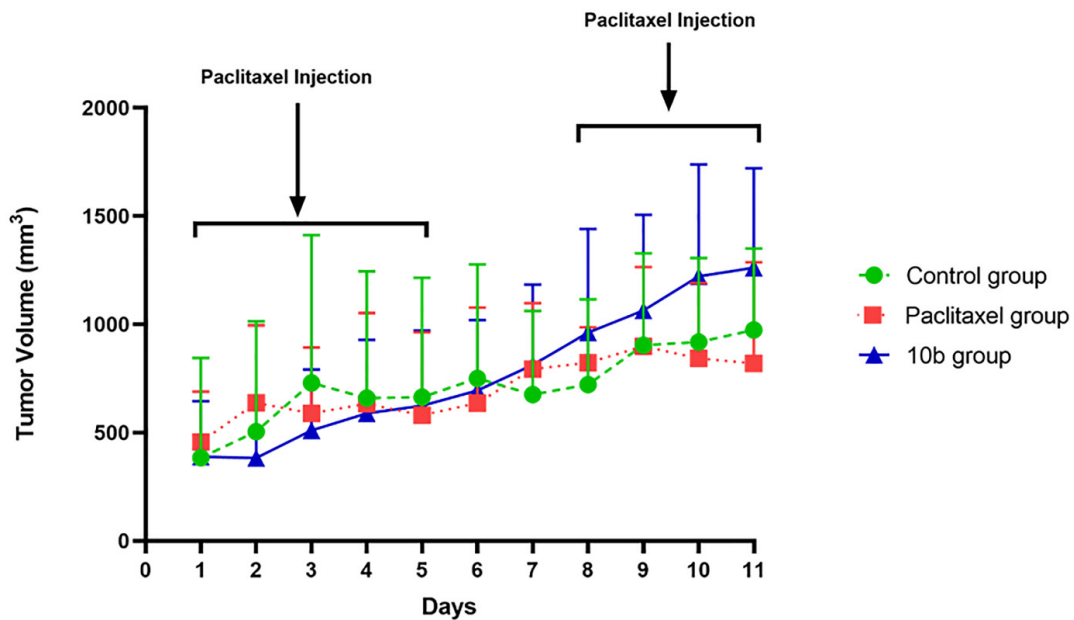


Figure 5. The results of measuring the size of the tumor in different groups studied and on different days (Mean \pm SE).

Mice survival analysis

As shown in Figure 6, in each of the paclitaxel and control groups, five mice died during the study. Interestingly, no mortality was observed in the group 10b. The survival rates of mice in control, paclitaxel and 10b groups were 50, 50 and 100%, respectively.

Tumor histopathology

Figure 7 shows the microphotography of the tumor mass in all groups. In the control group, the tissue structure of the tumor mass shows high mitotic division. Tissue necrosis is not seen except in the central part due to lack of nutrients reaching the cells. But in groups

paclitaxel and 10b, with high density nucleus of tumor cells and foamy vacuolated tumor cells are more common than in the control group. These changes are more evident in group paclitaxel than in group 10b. Quantitative evaluation showed that the rate of tumor tissue necrosis in the paclitaxel group increased significantly compared to the control group ($P < 0.001$). The rate of tumor tissue necrosis in group 10b was significantly increased compared to the control group ($P < 0.05$). In addition, the rate of tumor tissue necrosis was higher in the paclitaxel group than in the 10b group, but this increase was not statistically significant.

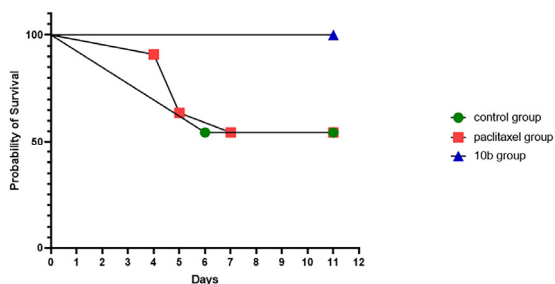


Figure 6. Mice mortality in the studied groups.

Liver pathology

Figure 8 shows the microphotography of the liver tissue in all groups. In the control group, the liver shows a normal structure (sinusoid, hepatocyte, kupffer cells). But in groups paclitaxel and 10b, hepatocyte necrosis, sinusoidal dilatation, proliferation of kupffer cells, congestion, and hemorrhage were seen. This injury was more severe in group paclitaxel than in group 10b. Quantitative evaluations showed that liver damage in the group receiving paclitaxel was significantly higher than in the control group ($P < 0.001$). Also, liver damage

in mice receiving compound 10b was significantly higher than in the control group ($P < 0.01$); But no statistically significant difference was observed between 10b and paclitaxel groups.

Cardiac pathology

Figure 9 shows the microphotography of the heart tissue in all groups. In the control group, the heart tissue shows a normal structure. But in groups paclitaxel and 10b, necrosis, infiltration of inflammatory cells, edema, eosinophilic myocytes and hemorrhage were seen. This injury was more severe in group paclitaxel than in group 10b. Quantitative evaluation showed that heart damage was significantly higher in both groups receiving paclitaxel and 10b compared to the control group ($P < 0.0001$). Also, heart damage was lower in mice receiving compound 10b compared to the paclitaxel group, but this reduction was not statistically significant.

Discussion

The 1,2,4-triazine ring is a widely used scaffold for many biologically active compounds, natural or synthetic, with a wide range of pharmacological effects.

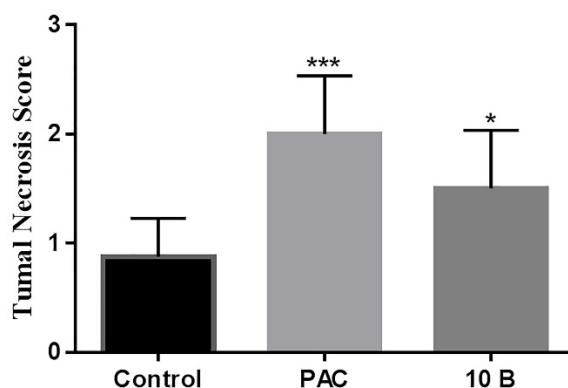
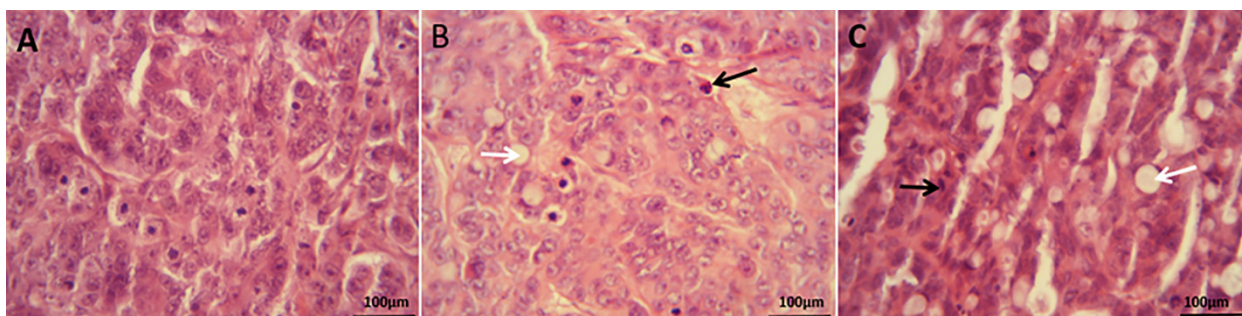


Figure 7. Results of tumor pathology in the studied groups. A) tissue sample from the control group. B) tissue sample from paclitaxel group and C) tissue sample from group 10b. Black arrow: with high density nucleus of tumor cells. White arrow: foamy vacuolated tumor cells. Hematoxylin and eosin staining. 20% magnification, load scale: 100 μ m.

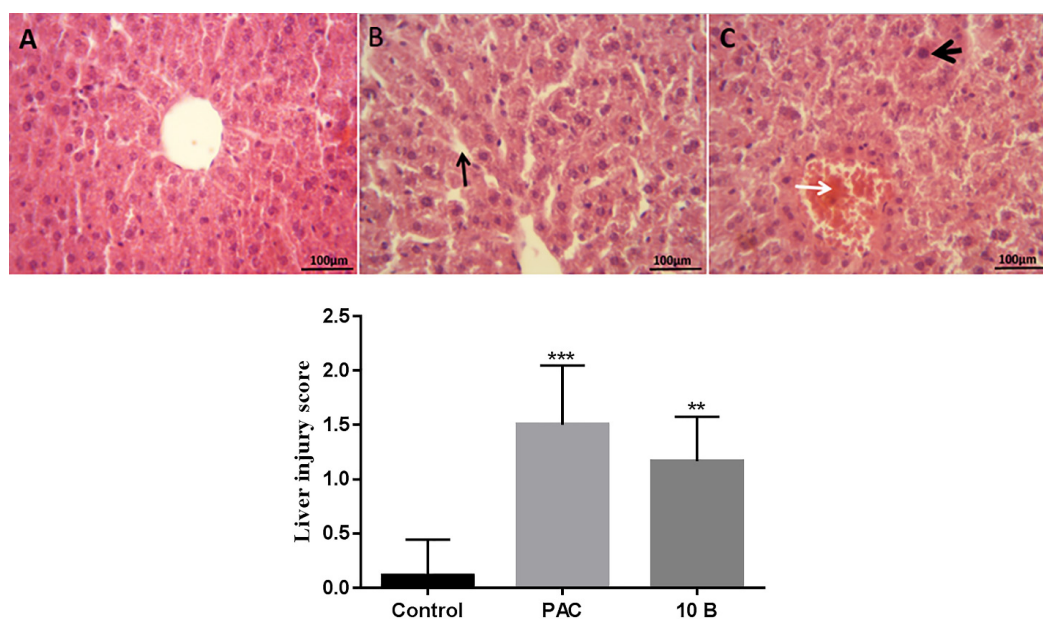


Figure 8. Results of liver tissue pathology. A) tissue sample from the control group. B) tissue sample from paclitaxel group and C) tissue sample from group 10b. Thin black arrow: Sinusoidal dilatation. Thick black arrow: Hepatocyte eosinophilia. White arrow: Lobular center venous congestion. Hematoxylin and eosin staining. 20% magnification, load scale: 100 μ m.

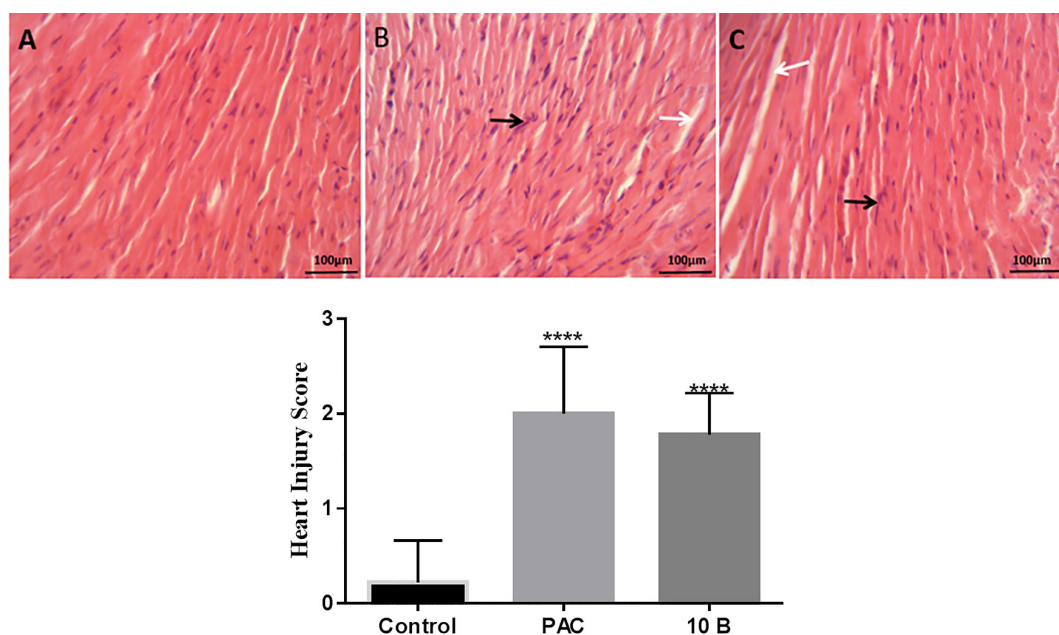


Figure 9. Results of heart tissue pathology. A) tissue sample from the control group. B) tissue sample from paclitaxel group and C) tissue sample from group 10b. Black arrow: Infiltration of inflammatory cells. White Arrow: Inflation. Hematoxylin and eosin staining. 20% magnification, load scale: 100 μ m

In particular, it is known as anti-tumor, anti-HIV, antimicrobial, anti-inflammatory, neuroprotective, anti-Alzheimer's. The NCNN sequence of 1,2,4-triazine ring is considered as an essential component for various pharmacological activities (15). The triazolotriazine

nucleus has been considered as a main interacting fragment in the design of the c-Met tyrosine kinase inhibitors because it has electron-deficiency due to the presence of the several nitrogen atoms. The electron-deficiency of the triazolotriazine nucleus makes it a

prominent motif to interact with the electron-rich Tyr1230 through a π - π stacking in the active site. This interaction infers affinity and selectivity to the c-Met inhibition (16). Accordingly, we investigated the *in vitro* and *in vivo* anti-cancer effect and cytotoxicity of our recently synthesized triazolotriazine derivative, 3-((Pyridin-4-ylmethyl)thio)-6-(p-tolyl)-[1,2,4]triazolo[4,3-b][1,2,4]triazine (10b) in HT-29 colon cells and tumor-induced nude mice.

The results of cellular MTT assay showed that increasing the dose of paclitaxel is associated with elevated cell mortality. In addition, the IC_{50} of paclitaxel was 0.86 and 0.34 μ M after 48 and 72 hours, respectively. Increasing the dose of compound 10b also increased cell mortality and the IC_{50} of this compound after 48 and 72 hours was 17.50 and 8.92 μ M, respectively. The results indicate that paclitaxel was more effective than 10b in inducing cell death. The potential of paclitaxel on increasing cancer cell mortality was 23 times greater than that of the 10b.

The results obtained from measuring the size of the tumors showed that there was no significant change in comparison between the control, paclitaxel and **10b** groups. This means that none of the two drugs were successful in inhibiting the growth of the colon tumor size in mice. Probably, this failure was due to the inappropriately chosen dosage regimens either in the drug concentration or the length of time for the drug consumption.

The results of measuring the weight of mice did not show any significant change between the three groups. This means that neither of the two compounds paclitaxel and **10b** had a significant effect on the mice weight.

Enlargement of the tumor led to necrosis of cells in the central part of the tumor mass. But in the tumor cells of the mice that received 10b and paclitaxel, vacuolation and nucleation of the nucleus were seen. Also, fibrous fibers in the structure of the tumor tissue in mice receiving 10b and paclitaxel were more than the control group. All of these tumor tissue alterations indicated that paclitaxel and 10b exhibited anti-tumor activity.

The histopathological examinations were performed for side effects induced by paclitaxel and 10b in normal tissues in mice. The tissue structure of the liver lobules in the control group was completely normal. Changes in the liver structure of mice receiving paclitaxel including lobular central venous congestion, Kupffer cell proliferation, sinusoidal dilatation, and eosinophilic hepatocytes were evident of the tissue damage. While, these changes were less severe in the group receiving **10b**. Cardiac muscle fibers in the control group had a normal structure. Infiltration of polymorphonuclear cells, activated fibroblasts, and edema were seen in the

heart structure of mice receiving paclitaxel. These changes were also seen in group 10b with less severity. According to the observations, the extent of hepatotoxicity and cardiac toxicity in mice receiving 10b was lower than that of the paclitaxel group.

Mortality rates were high in the control and paclitaxel treated mice as compared to 10b group. It is meant that tumor bearing mice died in the control and paclitaxel groups due to the enlargement of the tumor and its side effects, while the mortality rate was zero in 10b treated mice. It is cleared that 10b exhibited no significantly tumor growth inhibition whereas tumor histopathological findings and survival assessment were promising for 10b in this study.

Several studies have been reported considering the *in vivo* efficacy of some similar triazolotriazine derivatives on the xenograft tumor growth. Correspondingly, compound **1** (Figure 10) was identified as a highly potent compound with IC_{50} values of 0.24, 0.85, and 0.46 nM in the c-Met enzymatic activity, cellular activity in EBC-1 lung cell line, and MKN45 gastric cell line, respectively. *In vivo* usage of compound **1** at 25 mg/kg showed remarkable antitumor activity in c-Met-driven EBC-1 and MKN45 xenograft models with an inhibitory rate of 96.5%. Besides, oral administration of compound **1** at a 25 mg/kg dose led to complete tumor regression in the EBC-1 xenograft mouse model with minimal toxicity(16). Compound **2** is an exclusively selective c-Met inhibitor with IC_{50} of 0.006 μ M. This compound was tested for tumor growth inhibition (TGI) and its relationship to the inhibition of the c-Met autophosphorylation in a c-Met amplified GTL-16 xenograft tumor model. In efficacy studies for compound **2**, no weight loss was observed at any dose level. Tumor regression (-34% TGI) was seen with a dose of 100 mg/kg, and tumor stasis (100% TGI) was achieved at 30 mg/kg. Although compound **2** was a potent inhibitor of the c-Met receptor tyrosine kinase with high protein kinase selectivity, its broad phosphodiesterase family inhibition resulted in myocardial degeneration in rats, therefore it was terminated as a preclinical candidate(17). Compound **3** (SGX523) is extremely selective for c-Met with an IC_{50} of 4 nM and is orally bioavailable in all species tested, making it a useful tool for investigating the role of c-Met in animal models. Therefore, compound **3** was administrated to nude mice with established tumors to see whether this compound is sufficient to control the growth of xenografts derived from U87MG human glioblastoma cells and H441 human lung carcinoma cells. Administration of compound **3** at a dose of 30 mg/kg led to apparent tumor regression of U87MG. Additionally, the growth

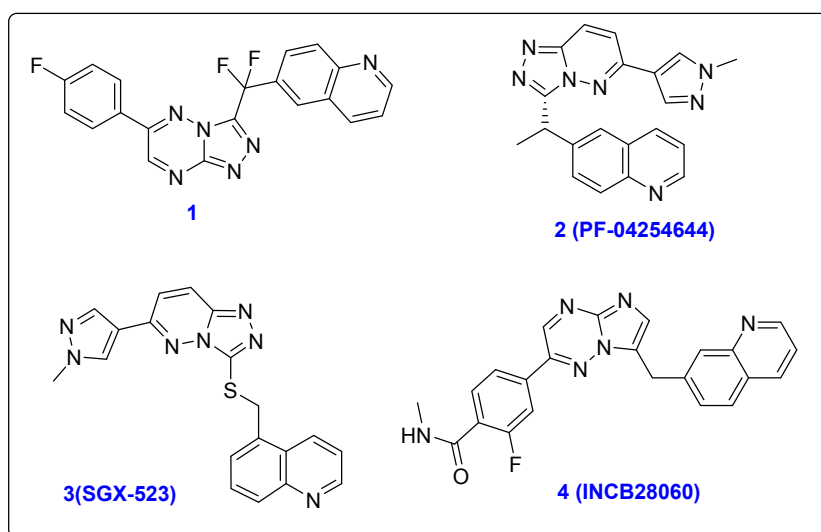


Figure 10. The representative selective c-Met inhibitors with antitumor activity.

of H441 tumors in mice treated with compound **3** at 30 mg/kg reduced tumor c-Met autophosphorylation levels. Unfortunately, a phase I clinical trial to assess the safety of SGX523 had to be stopped due to kidney toxicity(18). Compound **4** (INCB28060) is a new c-Met inhibitor with an IC_{50} of 0.13 nM in a cell-based assay and more than 10,000-fold selectivity against a broad panel of human kinases. The S114 cell-derived mouse tumor model (S114 cell line stably expresses human HGF and c-MET) was used to evaluate *in vivo* activities of compound **4**. Treatment with small molecule **4** at 0.3 mg/kg led to nearly 50% inhibition of c-Met phosphorylation. Oral administration of this compound inhibited c-Met phosphorylation and tumor growth in c-Met-driven mouse tumor models in a time- and dose-dependent manner, with no evidence of toxicity or weight loss(19).

Totally, the results of the previous studies indicate that toxicity evaluation of the drugs is an integral part of the lead optimization process and *in vivo* safety profile of a drug-like compound assures that the entire process will proceed almost with confidence.

Conclusion

In this study, we evaluated the potential of compound **10b** as an anti-cancer agent on HT-29 colon cells and HT-29 xenograft nude mice. *In vitro* assays showed that compound **10b** is an effective inhibitor for HT-29 cancer cell lines with IC_{50} = 8.92 μ M, compared to the standard drug paclitaxel (IC_{50} = 0.34 μ M). No apparent toxicity in weight loss and morbidity was observed with the administration of **10b** in mice, revealing acceptable safety. Happily, the extent of

hepatotoxicity and cardiac toxicity in mice receiving **10b** was lower than that of the paclitaxel group. These findings suggested that compound **10b** is unlikely to exert severe unfavorable effects in host organs and tissues at therapeutically relevant doses. Although, **10b** failed to considerably reduce tumor size, but its high survival potential in mice receiving **10b** and tumor histopathological findings were promising in this study.

Human and Animal Rights

All experiments were accomplished in accordance with the ethical standards and protocols approved by the Committee of Animal Experimentation of Mazandaran University of Medical Sciences, Sari, Iran (Ethics Code: IR.MAZUMS.REC.1397.4831).

Acknowledgment

This study was accomplished through grant number 4831 from the Mazandaran University of Medical Sciences, Sari, Iran.

Conflict of interest

Authors declare no conflict of interest.

References

1. Fitzmaurice C, Abate D, Abbasi N, Abbastabar H, Abd-Allah F, Abdel-Rahman O, et al. Global, Regional, and National Cancer Incidence, Mortality, Years of Life Lost, Years Lived With Disability, and Disability-Adjusted

- Life-Years for 29 Cancer Groups, 1990 to 2017: A Systematic Analysis for the Global Burden of Disease Study. *JAMA Oncol.* 2019 Dec;5(12):1749–68.
- Sung H, Ferlay J, Siegel RL, Laversanne M, Soerjomataram I, Jemal A, et al. Global cancer statistics 2020: GLOBOCAN estimates of incidence and mortality worldwide for 36 cancers in 185 countries. *CA Cancer J Clin.* 2021;71(3):209–49.
 - López-Lázaro M. The stem cell division theory of cancer. *Crit Rev Oncol Hematol.* 2018;123:95–113.
 - Noori-Dalooi MR, Ebadi N. Pharmacogenomics and cancer stem cells. *Med Sci J Islam Azad University-Tehran Med Branch.* 2015;25(1):1–15.
 - Buczacki SJA, Popova S, Biggs E, Koukorava C, Buzzelli J, Vermeulen L, et al. Itraconazole targets cell cycle heterogeneity in colorectal cancer. *J Exp Med.* 2018;215(7):1891–912.
 - Cesaro P, Raiteri E, Demoz M, Castino R, Baccino FM, Bonelli G, et al. Expression of protein kinase C β 1 confers resistance to TNF α -and paclitaxel-induced apoptosis in HT-29 colon carcinoma cells. *Int J cancer.* 2001;93(2):179–84.
 - Bottaro DP, Rubin JS, Faletto DL, Chan AM-L, Kmieciak TE, Vande Woude GF, et al. Identification of the hepatocyte growth factor receptor as the c-met proto-oncogene product. *Science* (80-). 1991;251(4995):802–4.
 - Cooper CS, Park M, Blair DG, Tainsky MA, Huebner K, Croce CM, et al. Molecular cloning of a new transforming gene from a chemically transformed human cell line. *Nature.* 1984;311(5981):29–33.
 - Gherardi E, Birchmeier W, Birchmeier C, Woude G Vande. Targeting MET in cancer: rationale and progress. *Nat Rev cancer.* 2012;12(2):89–103.
 - Takeuchi K, Ito F. Receptor tyrosine kinases and targeted cancer therapeutics. *Biol Pharm Bull.* 2011;34(12):1774–80.
 - Zhang Y, Xia M, Jin K, Wang S, Wei H, Fan C, et al. Function of the c-Met receptor tyrosine kinase in carcinogenesis and associated therapeutic opportunities. *Mol Cancer.* 2018;17(1):1–14.
 - Dadashpour S, Küçükılınç TT, Ayazgök B, Hosseinimehr SJ, Chippindale AM, Foroumadi A, et al. Discovery of novel 1,2,4-triazolo-1,2,4-triazines with thiomethylpyridine hinge binders as potent c-Met kinase inhibitors. *Future Med Chem [Internet].* 2019 May;11(10):1119–36. Available from: <https://www.future-science.com/doi/10.4155/fmc-2018-0412>
 - Rezaie-Tavirani M, Fayazfar S, Heydari-Keshel S, Rezaee MB, Zamanian-Azodi M, Rezaei-Tavirani M, et al. Effect of essential oil of *Rosa Damascena* on human colon cancer cell line SW742. *Gastroenterol Hepatol from bed to bench.* 2013;6(1):25.
 - Tomayko MM, Reynolds CP. Determination of subcutaneous tumor size in athymic (nude) mice. *Cancer Chemother Pharmacol.* 1989;24(3):148–54.
 - Khatir ZZ, Irannejad H. Pharmacologic Activities of 5, 6-Diaryl/heteroaryl-3-substituted-1, 2, 4-triazines as a Privileged Scaffold in Drug Development. *Mini Rev Med Chem.* 2021;21(19):2874–928.
 - Zhan Z, Peng X, Liu Q, Chen F, Ji Y, Yao S, et al. Discovery of 6-(difluoro (6-(4-fluorophenyl)-[1, 2, 4] triazolo [4, 3-b][1, 2, 4] triazin-3-yl) methyl) quinoline as a highly potent and selective c-Met inhibitor. *Eur J Med Chem.* 2016;116:239–51.
 - Cui JJ, Shen H, Tran-Dubé M, Nambu M, McTigue M, Grodsky N, et al. Lessons from (S)-6-(1-(6-(1-Methyl-1 H-pyrazol-4-yl)-[1, 2, 4] triazolo [4, 3-b] pyridazin-3-yl) ethyl) quinoline (PF-04254644), an Inhibitor of Receptor Tyrosine Kinase c-Met with High Protein Kinase Selectivity but Broad Phosphodiesterase Family Inhibit. *J Med Chem.* 2013;56(17):6651–65.
 - Buchanan SG, Hendle J, Lee PS, Smith CR, Bounaud P-Y, Jessen KA, et al. SGX523 is an exquisitely selective, ATP-competitive inhibitor of the MET receptor tyrosine kinase with antitumor activity in vivo An Exquisitely Selective Kinase Inhibitor. *Mol Cancer Ther.* 2009;8(12):3181–90.
 - Liu X, Wang Q, Yang G, Marando C, Koblisch HK, Hall LM, et al. A Novel Kinase Inhibitor, INCB28060, Blocks c-MET--Dependent Signaling, Neoplastic Activities, and Cross-Talk with EGFR and HER-3 INCB28060, a c-MET Kinase Selective Inhibitor. *Clin cancer Res.* 2011;17(22):7127–38.